JOURNAL OF BACTERIOLOGY, May 2008, p. 3622–3631 Vol. 190, No. 10
0021-9193/08/$08.00+0 doi:10.1128/JB.00165-08

Catalytic Mechanism of Cyclic Di-GMP-Specific Phosphodiesterase: a Study of the EAL Domain-Containing RocR from *Pseudomonas aeruginosa*▽

Feng Rao,[1] Ye Yang,[2] Yaning Qi,[1] and Zhao-Xun Liang[1]*

Division of Chemical Biology and Biotechnology[1] and Division of Computational and Structural Biology,[2] School of Biological Sciences, Nanyang Technological University, 60 Nanyang Drive, Singapore 637551, Republic of Singapore

Received 1 February 2008/Accepted 4 March 2008

EAL domain proteins are the major phosphodiesterases for maintaining the cellular concentration of second-messenger cyclic di-GMP in bacteria. Given the pivotal roles of EAL domains in the regulation of many bacterial behaviors, the elucidation of their catalytic and regulatory mechanisms would contribute to the effort of deciphering the cyclic di-GMP signaling network. Here, we present data to show that RocR, an EAL domain protein that regulates the expression of virulence genes and biofilm formation in *Pseudomonas aeruginosa* PAO-1, catalyzes the hydrolysis of cyclic di-GMP by using a general base-catalyzed mechanism with the assistance of Mg^{2+} ion. In addition to the five essential residues involved in Mg^{2+} binding, we propose that the essential residue E_{352} functions as a general base catalyst assisting the deprotonation of Mg^{2+}-coordinated water to generate the nucleophilic hydroxide ion. The mutation of other conserved residues caused various degree of changes in the k_{cat} or K_m, leading us to propose their roles in residue positioning and substrate binding. With functions assigned to the conserved groups in the active site, we discuss the molecular basis for the lack of activity of some characterized EAL domain proteins and the possibility of predicting the phosphodiesterase activities for the vast number of EAL domains in bacterial genomes in light of the catalytic mechanism.

Cyclic di-GMP was first discovered as a regulator of cellulose synthesis in *Glucoacetobacter xylinus* and is emerging as a major bacterial second messenger (14, 27, 28, 37). The intracellular concentration of cyclic di-GMP is controlled by the GGDEF domain proteins with diguanylate cyclase (DGC) activity and the EAL domain proteins with cyclic di-GMP-specific phosphodiesterase activity (27). GGDEF domains catalyze the condensation of two molecules of GTP to generate cyclic di-GMP, while the EAL domains catalyze the hydrolysis of cyclic di-GMP to generate the dinucleotide 5′-pGpG (Fig. 1). A family of HD-GYP domain proteins is also able to hydrolyze cyclic di-GMP to produce GMP (30), but the overwhelmingly large number of genes encoding the EAL domains in bacterial genomes suggests that they are the major phosphodiesterases responsible for maintaining the cellular cyclic di-GMP concentration.

Accumulating evidence suggests that EAL domain-containing proteins, including a large number of proteins that contain both the EAL and GGDEF domains, regulate a variety of cellular functions and phenotypes associated with bacterial infection. The regulation of virulence gene transcription, biofilm formation, motility, and adhesion has been reported in various pathogenic bacteria. Several proteins in the human pathogen *Vibrio cholerae*, including VieA and CdgC, have been implicated in biofilm formation, motility, and virulence factor production (15, 23, 40). An EAL domain protein was found to control lateral flagellar-gene expression and swarming behavior in *Vibrio parahaemolyticus* (17). In *Salmonella enterica*, the disruption of the EAL domain protein CdgR weakens bacterial resistance to hydrogen peroxide and accelerates bacterial killing by macrophages (12). In the opportunistic pathogen *Pseudomonas aeruginosa*, the EAL domain-containing protein FimX controls twitching motility and biofilm formation (13, 16) and the BifA protein controls biofilm formation and swarming (19). A systematic analysis of the GGDEF and EAL domain proteins in *P. aeruginosa* identified several other EAL domain proteins as being involved in virulence expression and biofilm formation (16, 20). Therefore, although the EAL domain proteins are not essential for the in vitro viability of pathogenic bacteria, they may be critical for the in vivo survival of the pathogens in host organisms, considering their roles in virulence expression and biofilm formation. This makes them potential targets for developing antibacterial agents that aim to neutralize virulence functions.

The genomes of the bacteria that contain cyclic di-GMP signaling networks generally encode multiple EAL domain proteins. For example, the genomes of *P. aeruginosa* PAO-1 and *V. cholerae* contain 21 and 32 open reading frames, respectively, for EAL domain proteins. In previous biochemical studies of EAL domain proteins, it was shown that Mg^{2+}, or Mn^{2+}, is required for the enzymes to hydrolyze cyclic di-GMP (31, 36, 38). It was also found that Zn^{2+} and Ca^{2+} can strongly inhibit the enzymatic activity, presumably by dislodging the Mg^{2+} ion. The Glu in the EAL (or EXL) signature motif seems to be essential for the enzymatic activity, because the E→A mutations in two EAL domain proteins abolished their

* Corresponding author. Mailing address: Division of Chemical Biology and Biotechnology, School of Biological Sciences, Nanyang Technological University, 60 Nanyang Drive, Singapore 637551, Republic of Singapore. Phone: 65 63167866. Fax: 65 67913856. E-mail: zxliang@ntu.edu.sg.

▽ Published ahead of print on 14 March 2008.

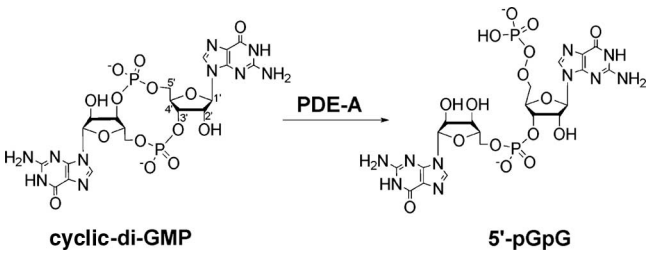

FIG. 1. Phosphodiesterase A (PDE-A) catalyzes hydrolysis of cyclic-di-GMP to generate the linear diguanylic acid 5′-pGpG.

phosphodiesterase activities (6, 38). Additionally, Schmidt and coworkers suggested that other conserved motifs, including a DDFGTG motif, may be essential for the catalytic activity (31). The phosphodiesterase activity of the EAL domain of CC3396 from *Caulobacter crescentus* can be stimulated by the binding of GTP to the adjacent enzymatically inactive GGDEF domain (6). A similar observation was reported for the protein FimX, involved in the regulation of twitching motion in *P. aeruginosa* (16). The utilization of the GGDEF domain could be a major strategy for regulating the catalytic activity of EAL domains, considering the large number of proteins that contain the GGDEF-EAL didomain. Meanwhile, the widespread occurrence of GGDEF-EAL domains also raises the possibility that some EAL domains may function as regulatory rather than catalytic domains. However, due to limited information about the catalytic mechanism of EAL domains, such a distinction has remained speculative.

RocR was identified as a response regulator in the RocSAR (or SadARS) two-component signaling system in *P. aeruginosa* (18, 21, 29). RocSAR consists of the histidine kinase RocS1 and two response regulators, RocA1 and RocR. The RocSAR system controls bacterial biofilm formation and virulence gene expression by regulating the transcription of various genes, including the *cup* fimbrial-gene clusters and type III secretion system genes (18, 20, 21). Deduced from the protein sequence, RocR contains an N-terminal CheY-like phosphoryl receiver domain and a C-terminal EAL domain. It was postulated that RocR negatively regulates the expression of *cup* genes by antagonizing the activity of RocA1, which is a typical response regulator with a DNA-binding domain (21). The detailed molecular mechanism for this antagonism is not known at present, though it has been speculated that the EAL domain may function as a regulatory domain lacking phosphodiesterase activity. Here, we present biochemical data to demonstrate that the EAL domain of RocR is catalytically active, with cyclic di-GMP-specific phosphodiesterase activity. Using RocR as a model system, we carried out systematic mutagenesis in the EAL domain to probe the roles of 14 conserved polar residues in catalysis. Based on the biochemical data and aided by the crystal structure of a homologous EAL domain protein, we assigned functions to the conserved residues and proposed a general base-catalyzed mechanism with the assistance of the Mg^{2+} ion. In the context of the proposed catalytic mechanism, we rationalize the inactivity of some characterized EAL domains and discuss the possibility of predicting the phosphodiesterase activities of EAL domains based on protein sequences.

MATERIALS AND METHODS

Protein cloning, expression, and purification. The genomic DNA of *P. aeruginosa* PAO-1 (ATCC) was isolated following standard procedures. The genes PA3702, PA3947, PA0290, and PA2567, encoding the WspR, RocR, PA290, and PA2567 proteins, respectively, were amplified by PCR using the Expand High-Fidelity Kit (Roche). The amplified DNA fragments were cloned into the expression vector pET-26(b+) (Novagen) with compatible restriction sites. The plasmids harboring the gene and the His_6 tag-encoding sequence were transformed into *Escherichia coli* strain BL21(DE3). For protein expression, 1 liter of bacterial culture (LB medium) was grown to an optical density of 0.8 before being induced with 0.8 mM isopropyl-β-D-thiogalactopyranoside. The culture was shaken at 16°C for ~12 h before being pelleted by centrifugation. The cells were lysed in 20 ml lysis buffer (20 mM Tris [pH 8.0], 500 mM NaCl, 5% glycerol, 0.1% β-mercaptoethanol, 0.1% Triton X-100, and 1 mM phenylmethylsulfonyl fluoride). After centrifugation at 25,000 rpm for 30 min, the supernatant was filtered and then incubated with 2 ml of Ni^{2+}-nitrilotriacetic acid resin (Qiagen) for 1 h at 4°C. The resin was washed with 50 ml of W1 buffer (lysis buffer with 20 mM imidazole) and 20 ml of W2 buffer (lysis buffer with 50 mM imidazole). The proteins were eluted using a stepped gradient method with the elution buffer containing 20 mM Tris (pH 8.0), 500 mM NaCl, 5% glycerol, and 200 mM, 300 mM, or 500 mM imidazole. After sodium dodecyl sulfate-polyacrylamide gel electrophoresis analysis, fractions with purities higher than 95% were pooled and desalted using a PD-10 column (GE Healthcare). The proteins were first concentrated using an Amicon concentrator (Millipore) and dialyzed in the storage buffer (50 mM Tris buffer [pH 8.0], 250 mM NaCl, 25 mM KCl, 5 mM $MgCl_2$, 40% glycerol, 1 mM dithiothreitol). The proteins were stored at −20°C after measurement of the protein concentration by Bradford assay. All RocR mutants were generated using the Site-Directed Mutagenesis II Kit (Stratagene) according to the manufacturer's instruction manual. Mutations were verified using a BigDye Terminator v3.1 cycle-sequencing kit on an ABI Prism 3100 Genetic Analyzer (Applied Biosystems). Mutant proteins were expressed, purified, and stored under the same conditions. The yield of the recombinant protein was 10 to 15 mg/liter for the wild-type RocR and the mutants, except for the E268Q mutant (~1 mg/liter).

Enzymatic synthesis of cyclic di-GMP. Cyclic di-GMP was produced enzymatically by using WspR and PA290, two DGC domain-containing proteins encoded by the genes PA3702 and PA0290 in *P. aeruginosa* PAO-1. The progress of cyclic di-GMP synthesis was monitored by using an Agilent LC1200 system (mobile phase, 20 mM triethylammonium bicarbonate [pH 7.0], 10% methanol, 0.6 ml/min) with an XDB C_{18} column (4.6 by 150 mm). Cyclic di-GMP was synthesized by incubating the enzymes and GTP (Sigma) at 30°C in a 10-ml reaction mixture that contained 50 mM Tris buffer (pH 7.6), 20 mM $MgCl_2$, and 0.5 mM EDTA. The enzymes were supplemented in batch to maximize turnover. The reaction was stopped by boiling the reaction mixture for 5 min after ~75% of the GTP was converted to cyclic di-GMP as estimated by high-performance liquid chromatography (HPLC) analysis. Following centrifugation at 14,000 rpm for 4 min to remove the protein precipitate, the supernatant was filtered and loaded onto the Eclipse XDB C_{18} (9.4- by 250-mm) column for purification of cyclic di-GMP. The cyclic di-GMP was eluted using the same mobile phase described above. The fractions that contained cyclic di-GMP were pooled and evaporated to yield the white powder, which was dissolved in 5 mM Tris buffer (pH 7.0) for storage. The identity of cyclic di-GMP was confirmed by matrix-assisted laser desorption ionization mass spectrometry with a molecular weight (MW) of 690.085 (calculated MW, 690.09). The concentration of the stock solution was determined by using a UV-Vis spectrophotometer (Shimadzu). The extinction coefficient (ε_{260}) of 26,100 optical density units M^{-1} cm^{-1} was used for the calculation of the cyclic-di-GMP concentration (44).

Measurement of kinetic parameters. The identity of the product 5′-pGpG was confirmed by matrix-assisted laser desorption ionization mass spectrometry with an MW of 708.108 (calculated MW, 708.11). The measurement of steady-state kinetic parameters was carried out by monitoring the formation of the product 5′-pGpG using HPLC. The standard assay was set up as follows: 100 mM Tris buffer (pH 8.0) with 20 mM KCl and 25 mM $MgCl_2$. Reactions were stopped by adding 1/10 volume of 1 M $CaCl_2$ and heating the mixture at 95°C for 5 min. After the protein precipitate was removed by centrifugation, the supernatant was loaded onto HPLC for quantification. The initial velocity at a certain substrate concentration was obtained from a series of reactions with varying incubation times. The total turnover was kept below 10% to ensure the accurate measurement of initial velocities within the linear range. The initial velocity was measured at 6 to 12 substrate concentrations. The kinetic parameters k_{cat} and K_m were obtained by fitting the initial velocities at various substrate concentrations to the Michaelis-Menten equation using the software Prism (GraphPad).

pH dependence and data fitting. To cover the pH 6.2 to 9.5 range, 100 mM Bis-Tris (pH 6.0 to 6.9), Tris (pH 7.0 to 9.0), or CHES [2-(cyclohexylamino)ethanesulfonic acid] (pH 9.0 to 9.5) buffer with 20 mM KCl and 25 mM $MgCl_2$ was used for kinetic measurement to obtain the pH profiles for RocR and the mutant E352Q. The precise pH of the reaction mixture was measured using a micro-pH electrode. The initial velocities (V_{max}) at two saturating cyclic di-GMP concentrations (25 and 30 μM) were measured at various pH values. No significant difference was observed for V_{max}, and only one set of the data was used for calculating the k_{cat} values used in the pH profiles. Given the observed bell-shaped pH profiles, a simplified model containing two ionizable catalytic groups was used to describe the pH dependence. (Mg^{2+})E-S, (Mg^{2+})EH-S, and (Mg^{2+})EH_2-S represent the different ionization states of the ternary complex containing E (enzyme), Mg^{2+}, and S (substrate). K_{a1} and K_{a2} are the ionization constants for the two groups that undergo ionization within the pH range of 6.2 to 9.5.

$$(Mg^{2+})\text{E-S} \overset{K_{a1}}{\rightleftharpoons} (Mg^{2+})\text{EH-S} \overset{K_{a2}}{\rightleftharpoons} (Mg^{2+})\text{EH}_2\text{-S}$$

$$\downarrow k_{cat}$$

$$(Mg^{2+})\text{EH-P}$$

$$\downarrow$$

$$(Mg^{2+})\text{EH} + \text{P}$$

Based on the model, the bell-shaped pH profiles were fitted to equation 1 below to obtain pK_{a1} and pK_{a2}, the apparent pK_a values for the two ionizable groups, using the software DataFit (Oakdale Engineering).

$$\log(k_{cat}) = \log\left(\frac{k_{cat}(\max)}{1 + 10^{(pK_{a2} - pH)} + 10^{(pH - pK_{a1})}}\right) \quad (1)$$

Size exclusion chromatography. Gel filtration was performed at 4°C using the Akta fast-protein liquid chromatography system equipped with a Superdex 200 HR 16/60 column (GE Healthcare). The buffer used for gel filtration was comprised of 20 mM Tris-HCl (pH 8.0), 0.5 M NaCl, 5% glycerol, and 0.5 mM dithiothreitol. The molecular mass was estimated based on the standard curve generated by using the standard proteins ferritin (440 kDa), aldolase (158 kDa), conalbumin (75 kDa), ovalbumin (44 kDa), and blue dextran (for void volume determination).

Structure modeling and computational docking. The structural model for the EAL_{RocR} domain was constructed using the Swiss-Model server with the coordinates of tdEAL structure (Protein Data Bank [PDB] code 2R6O) as a template. The E value (3.8×10^{-31}) of the model was extremely low, and more than 95% of the residues fell into the favorable region in a Ramachandran plot. AutoDock 4 was used for the docking of cyclic di-GMP onto the receptor tdEAL (chain A) (10). Structural optimization and pK_a calculation were carried out to determine the protonation state using PDB2PQR (8, 22). Formal and partial charges were then assigned by the command line tool in Autodock Tools. Mg^{2+} ion was incorporated into the PDBQT files with a charge of +1.2, +1.4, or +1.6 to represent different hydrated statuses of the Mg^{2+} ion. The coordinates of cyclic di-GMP were taken from the PDB (PDB ID, 2RDE). Hydrogen atoms were added using Ghemical software (http://www.uku.fi/~thassine/projects/ghemical/), and charges were assigned similarly to the method described for the receptor. Chemical affinity and electrostatics maps were computed and centered near the metal ion with 70 by 70 by 70 grid points covering the putative binding cavity of the receptor with a spacing of 0.375 Å. Docking was performed using the Lamarckian genetic algorithm with the pseudo-Solis and Wets local-search method. The preliminary efforts to dock cyclic di-GMP monomer and dimer into the binding pocket failed to produce any meaningful result, likely due to the closed conformation adopted by a capping helix. Instead, we used a truncated version of cyclic di-GMP without the two guanine bases for docking. The docking generated a single set of conformations with the ligand residing in the substrate binding pocket with a 2-Å root mean-square deviation. The two guanine residues were then added back to the truncated cyclic di-GMP. The enzyme-Mg^{2+}-substrate ternary complex was subjected to molecular-dynamics simulation to generate the final docking model.

RESULTS

Size exclusion chromatography suggested that RocR is mainly a tetramer in solution with an apparent molecular mass of ~170 kDa (calculated mass, 176.4 kDa). RocR readily hydrolyzes cyclic di-GMP to produce 5′-pGpG, while no hydrolysis was observed for cyclic AMP and cyclic GMP, suggesting that the EAL_{RocR} domain is a cyclic-di-GMP-specific phosphodiesterase. Similar to other reported EAL domain proteins, Mn^{2+} ion can replace Mg^{2+} ion in catalysis, while Ca^{2+} and Zn^{2+} ions inhibit the phosphodiesterase activity. Under the experimental conditions, no substrate or product inhibition was observed for RocR. RocR catalyzes the hydrolysis of cyclic di-GMP with a k_{cat} of 0.67 ± 0.03 s^{-1} and a K_m of 3.2 ± 0.3 μM, which is close to the estimated cyclic-di-GMP cellular concentrations in *C. crescentus* (1.2 ± 0.11 μM) and in *Acetobacter xylinum* (5 to 10 μM) (6, 42).

While this work was in progress, the crystal structures (PDB codes 2BAS and 2R6O) for two putative cyclic-di-GMP-specific phosphodiesterases were determined by the Midwest Center for Structural Genomics (http://www.mcsg.anl.gov). Neither in vitro nor in vivo phosphodiesterase activity has been confirmed for either protein. The protein tdEAL (PDB ID, 2R6O) from *Thiobacillus denitrificans* contains a single EAL domain, while the protein YkuI (PDB ID, 2BAS) from *Bacillus subtilis* consists of an N-terminal EAL domain (EAL_{YkuI}) and a C-terminal domain with unknown function. Given the sequence similarity (53%) between EAL_{RocR} and tdEAL, we constructed a structural model for EAL_{RocR} by using the structure of tdEAL as a template. Overall, the model adopts the same $(\alpha/\beta)_8$ barrel fold and can be superimposed onto the crystal structure of tdEAL with a root mean-square deviation of 1.5 Å (backbone). Importantly, the side chain conformations of the conserved residues in the active site of tdEAL are preserved in the structural model of EAL_{RocR}. The structural model should be reasonably reliable for identifying catalytic residues, considering that most residues in the putative substrate binding pocket are conserved.

Site-directed mutagenesis and kinetic measurement. Sequence alignment of EAL domains (pfam 00563 software [Pfam is a web-based software (http://pfam.sanger.ac.uk/family?acc=PF00563]) in bacterial genomes revealed 14 conserved polar residues: 8 acidic residues (E_{175}, E_{265}, E_{268}, D_{295}, D_{296}, D_{318}, E_{352}, and E_{355}), 2 basic residues (R_{179} and K_{316}), and 4 neutral residues (Q_{161}, Q_{372}, N_{233}, and T_{267}). The 14 residues, which likely include the catalytically important residues, such as the Glu residue (E_{175}) from the EAL signature motif, are completely conserved in EAL_{RocR} and tdEAL. As seen in the model of EAL_{RocR} (Fig. 2), most of the 14 conserved residues reside on the C-terminal ends of the central β-barrel, with the exception of E_{175}, R_{179}, Q_{161}, and E_{265}, which are situated in the middle of β-strands. E_{268} and E_{355} are located outside of the central barrel and are referred as distal residues. E_{268} is the only residue among the 14 with the side chain carboxylate group pointing away from the central barrel.

To probe their roles in catalysis, each of the 14 conserved residues was mutated individually to alanine. The steady-state kinetic parameters (k_{cat} and K_m) for the wild type and the 14 single mutants were measured under identical experimental conditions. As shown in Table 1, the mutation of seven residues (Q_{161}, R_{179}, T_{267}, D_{296}, D_{318}, E_{355}, and Q_{372}) caused various degrees of reduction in k_{cat}, ranging from a negligible 1.3-fold for E355A to 29.1-fold for R179A and 33.5-fold for D296A, suggesting that they play only minor or nonessential roles in catalysis. The K_m values for the mutants Q161A,

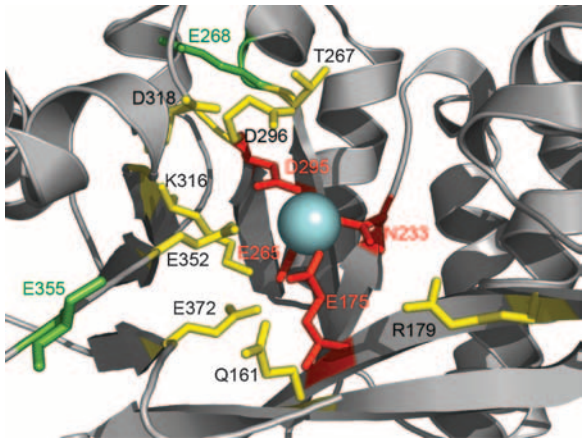

FIG. 2. Structural model of the EAL_{RocR} domain with the 14 conserved polar residues highlighted. The four residues for Mg^{2+} ion (sphere) binding are shown in red. The two distal residues are in green, whereas the rest of the conserved residues are in yellow.

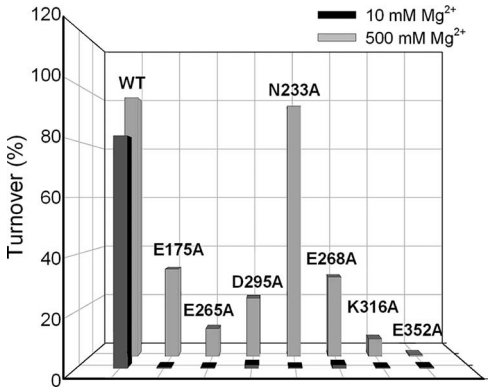

FIG. 3. Recovery of catalytic activity at elevated Mg^{2+} concentrations. The assay conditions were as follows: 100 mM Tris buffer (pH 8.0), 20 mM KCl, ~1.0 μM enzyme, 20 μM cyclic di-GMP, and 20-min incubation. WT, wild type.

R179A, and D296A were two- to threefold larger than that of the wild-type RocR, indicating that the three residues might be involved in substrate binding.

In sharp contrast, the mutation of the other seven residues, including E_{175}, N_{233}, E_{265}, E_{268}, D_{295}, K_{316}, and E_{352}, reduced the activity to below measurable level (>10^5-fold decrease). Loss of protein stability did not seem to account for the decrease in activity, because no noticeable precipitation or aggregation occurred during the protein purification and activity assay. The profound effects of the mutations suggested that these residues play essential roles in assisting catalysis or maintaining the structure of the active site. The seven residues will be referred to as essential residues from this point on. To further investigate whether the effects of the single mutations are due to structural perturbation, additional conservative mutants, E175Q, E265Q, D295N, E352Q, K316Q, and E268Q, were prepared. With the exception of E268Q, all of them showed activities slightly higher than or comparable to those of the corresponding alanine mutants, ruling out the possibility that the effects were caused by structural alteration and reinforcing the importance of the charge carried by the side chains. In contrast, the E268Q mutant exhibited significantly higher activity than the E268A mutant. Kinetic measurement revealed that the turnover number ($k_{cat} = 1.5 \times 10^{-3}$ s^{-1}) for E268Q was 446-fold lower than that of the wild-type RocR in contrast to the >10^5-fold decrease for the E268A mutant. Given its distal location, it is likely that E_{268} plays a pivotal structural rather than catalytic role. The exclusion of E_{268} as a catalytic residue left us with six essential residues for further investigation.

TABLE 1. Steady-state kinetic parameters for RocR and its mutants[a]

Enzyme	k_{cat} (s^{-1})	K_m (μM)	k_{cat}/K_m (s^{-1} μM^{-1})	Decrease in k_{cat} (fold)
RocR	0.67 ± 0.03	3.2 ± 0.3	0.21	
Q161A	0.13 ± 0.01	6.3 ± 1.0	$(2.1 \pm 0.4) \times 10^{-2}$	5.1
E175A	ND[b]			>10^5
R179A	$(2.3 \pm 0.1) \times 10^{-2}$	8.0 ± 0.9	$(2.9 \pm 0.3) \times 10^{-3}$	29.1
N233A	ND			>10^5
E265A	ND			>10^5
T267A	$(4.9 \pm 0.1) \times 10^{-2}$	2.2 ± 0.4	$(2.2 \pm 0.4) \times 10^{-2}$	13.4
E268A	ND			>10^5
E268Q	$(1.5 \pm 0.1) \times 10^{-3}$	0.3 ± 0.1	$(4.8 \pm 0.5) \times 10^{-3}$	446
D295A	ND			>10^5
D296A	$(2.1 \pm 0.3) \times 10^{-2}$	8.6 ± 2.8	$(2.7 \pm 0.9) \times 10^{-3}$	33.5
K316A	ND			>10^5
D318A	$(8.0 \pm 0.5) \times 10^{-2}$	5.9 ± 1.5	$(1.4 \pm 0.4) \times 10^{-2}$	8.4
E352A	ND			>10^5
E352C	ND			>10^5
E352Q	$(1.1 \pm 0.1) \times 10^{-5}$	3.8 ± 0.7	$(2.9 \pm 0.6) \times 10^{-6}$	6.1×10^4
E352D	$(2.2 \pm 0.1) \times 10^{-5}$	2.2 ± 0.5	$(1 \pm 0.2) \times 10^{-5}$	3.0×10^4
E355A	0.51 ± 0.07	2.6 ± 1.1	0.19 ± 0.09	1.3
Q372A	$(8.0 \pm 0.5) \times 10^{-2}$	1.3 ± 0.3	$(6.2 \pm 1.5) \times 10^{-2}$	8.4

[a] Conditions were 100 mM Tris buffer (pH 8.0) (23°C), 20 mM KCl, 25 mM $MgCl_2$.
[b] ND, not determined due to inactivity or extremely low activity (<10^5-fold less active than wild-type RocR).

Recovery of the catalytic activities of inactive mutants at high Mg^{2+} concentrations. Previous studies showed that the Mg^{2+} or Mn^{2+} ion is indispensable for the in vitro phosphodiesterase activities of EAL domains. Mg^{2+} is likely to be the metal ion utilized by EAL domains under physiological conditions. In the crystal structure of the homodimeric tdEAL, the residues corresponding to the four essential residues (E_{175}, E_{265}, D_{295}, and N_{233}) identified above coordinate one Mg^{2+} ion, along with two water ligands, in both subunits. Interestingly, in one subunit (2R6O; chain B), the other two conserved residues, D_{296} and D_{318}, coordinate a second Mg^{2+} ion and raise the possibility of a catalytic mechanism assisted by two metal ions.

The binding of the Mg^{2+} ion by the four residues (E_{175}, E_{265}, D_{295}, and N_{233}) in solution is supported by the observation that mutation of any of the four residues to alanine caused a drastic decrease in catalytic efficiency. Additionally, we examined the catalytic activities of the four mutants E175A, E265A, D295A, and N233A, along with three other inactive mutants, E268A, K316A, and E352A, at elevated Mg^{2+} concentrations. By using approximately the same amount of enzyme, we found that at elevated Mg^{2+} concentrations (up to 500 mM), the catalytic activity of N233A could be fully restored, and the activities of E175A, E265A, D295A, E268A, and K316A could be partially recovered, compared to the turnover of the wild-type enzyme at a 10 mM Mg^{2+} concentration (Fig. 3). These results dem-

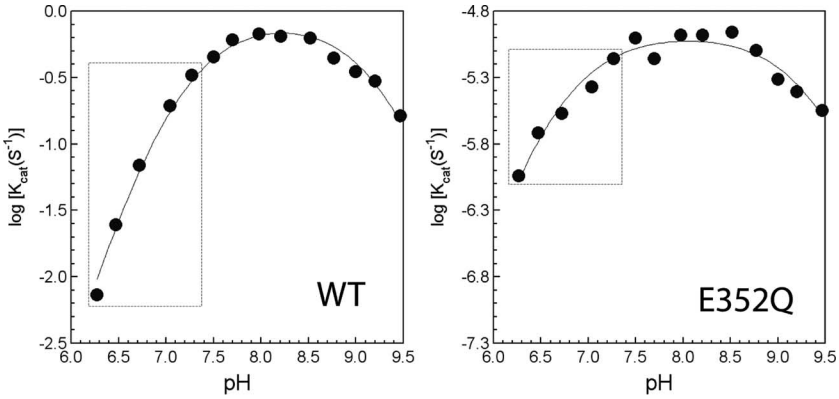

FIG. 4. pH dependence of enzymatic activity for wild-type (WT) RocR and the mutant E352Q. The curves were obtained from the nonlinear-least-square fitting of the data to equation 1 (see Materials and Methods).

onstrated that the Mg^{2+}-binding site in the mutants could be populated again at a high Mg^{2+} concentration, indicating that the lack of activity at low Mg^{2+} concentrations was due to reduced binding affinity for Mg^{2+}. The different degrees of recovery probably reflect the contributions of the residues in Mg^{2+} binding, with N_{233} contributing the least. Although K_{316} is not directly involved in Mg^{2+} binding, the partial recovery of activity for K316A can be rationalized, given that K_{316} forms hydrogen bonds with E_{175} and E_{265} and may be important for the positioning of the two residues for Mg^{2+} binding (Fig. 2). The partial restoration of the activity of E268A at high [Mg^{2+}] is intriguing and may reflect its indirect role in Mg^{2+} binding, as we discuss below. Negligible recovery of activity was observed for the mutant E352A, suggesting that the residue E_{352} plays an essential role other than Mg^{2+} binding.

As for the second Mg^{2+} ion observed in the crystal structure of tdEAL, it is bound by D_{295} and D_{318} on the protein surface, along with four water molecules to complete the octahedral geometry. However, the mutations D296A and D318A cause only 29- and 8-fold reductions in k_{cat}, respectively, in sharp contrast to the catastrophic effect of mutating the residues that bind the first Mg^{2+} ion. Considering that a high Mg^{2+} concentration (200 mM) was used in crystallization, the second Mg^{2+}-binding site could be a physiologically irrelevant observation resulting from the crystallization conditions. Instead, the elevated K_m for the mutants D296A and D318A suggested that they may play small roles in substrate binding.

Identification of the general base catalyst. Phosphodiesterases generally hydrolyze substrates by using metal ion and general acid/base catalysts for substrate and/or water activation. To identify the potential general acid/base catalyst, we carried out computational docking using the structure of tdEAL to explore the structure of the enzyme-Mg^{2+}-substrate complex (Fig. 5). The relevance of the docking model obtained is supported by the following observations. First, in the model, one of the phosphates of cyclic di-GMP is coordinated with the essential Mg^{2+} ion, with the anionic phosphate oxygen occupying a position initially occupied by a water ligand. Second, the conserved R_{63} (R_{179} in RocR) interacts with the second phosphate group of cyclic di-GMP in the model. The interaction between R_{63} and the substrate is consistent with the elevated K_m for mutant R179A. Last, and most importantly, the docking conformation of cyclic di-GMP predicts that the nucleophilic attack of the Mg^{2+}-bound hydroxide ion will generate 5′-pGpG, but not 3′-pGpG, as we discuss in detail below.

In the crystal structure of tdEAL, a water molecule coordinated by the Mg^{2+} ion is within hydrogen bond distance of the residues E_{239} and D_{182} (E_{352} and D_{295} in RocR) (see Fig. 5). In the model of the ternary complex, the water molecule is located near the electrophilic phosphorus center of cyclic di-GMP at a distance of 3.0 Å. Cyclic di-GMP is oriented in such a way that the O (water)-P (phosphate)-O_L (leaving group) angle approaches 180°. The linear alignment of the H_2O and leaving group led us to propose a general base-catalyzed mechanism in which E_{352} (but not D_{295}) functions as a general base catalyst for deprotonating the Mg^{2+} ion-coordinated water to generate a nucleophilic hydroxide ion. To further validate the role of E_{352}, we prepared two more mutants (E352C and E352D) in addition to the E352A and E352Q mutants. Similar to E352A, the activity of E352C was so low (a $>10^5$-fold decrease in k_{cat}) that the determination of the kinetic parameters became unrealistic. The lack of activity for E352C suggested that the nucleophilic character of the side chain is unimportant, given that Cys carries a strong nucleophilic group (SH). The other two mutants, E352Q and E352D, exhibited slightly higher activity than the E352A mutant, which allowed us to measure the kinetic parameters using a high concentration of enzyme. Both mutants showed $>10^4$-fold reduction in the k_{cat} relative to the wild-type RocR (Table 1), indicating that the precise positioning of the negative charge carried by the carboxylate group is crucial for efficient catalysis.

Determination of the pH dependence of catalytic activity would yield information regarding the mechanism and the general acid/base catalyst. The measurement of the turnover numbers (k_{cat}) for RocR in the pH range of 6.2 to 9.5 revealed a bell-shaped pH profile with an ascending limb in the low-pH region and a descending limb in the high-pH range (Fig. 4, left). A simple model that contained two ionizable groups was used to fit the pH dependence data, as described in Materials and Methods. The limiting slope of 1.8 for the ascending limb suggests that one or two groups needed to be deprotonated in the enzyme-Mg^{2+}-substrate ternary complex for efficient catalysis. The limiting slope of 0.7 was also observed for the descending limb in the high-pH region. To probe the relation-

ship between the pH dependence behavior and the ionization of E_{352}, we also determined the pH profile for the E352Q mutant (Fig. 4, right). Although a bell-shaped curve was also observed for the mutant with a similar descending slope of 0.6, the limiting slope for the ascending limb had changed from 1.8 for the wild-type RocR to 0.7 for the mutant. The change in slope of 1.1 indicated that the observed pH dependence in the low-pH region was largely attributable to the protonation/deprotonation of E_{352}. The weakened pH dependence for the mutant supported a mechanism in which the deprotonated E_{352} functions as a general base catalyst for deprotonating the water molecule. Although D_{295} may assist in the deprotonation of the water molecule by influencing the pK_a of H_2O, it is unlikely that D_{295} functions as the proton acceptor (general base), given its low pK_a resulting from Mg^{2+} binding. Similar pH dependence measurement was not carried out for the D295A or D295N mutant due to the extremely low activity.

Finally, we examined another protein, PA2567, to test whether the essential role of E_{352} was limited to RocR. PA2567 is predicted to contain three domains (GAF, GGDEF, and EAL) and represents a large number of proteins that contain the GGDEF-EAL didomain. The EAL domain was found to be catalytically active, with a k_{cat} of 0.39 ± 0.03 s^{-1}. The mutation of corresponding residues of E_{352} (E_{548}) to Q decreased the k_{cat} by more than 10^4-fold, consistent with the observation for RocR.

DISCUSSION

Given the large number of genes encoding EAL domain proteins in bacteria, understanding the regulation of EAL domains is essential for understanding the complex cyclic di-GMP signaling network. In addition to cellular compartmentalization and transcriptional regulation (37), EAL domains are regulated by a wide array of regulatory domains at the protein level. The elucidation of the catalytic mechanism for EAL domains would be the first step toward understanding the protein level regulatory mechanism. Our investigation, which focused on the catalytic mechanism of the EAL domain of RocR, shed light on the physiological function of RocR, as well as the general catalytic mechanism of EAL domains.

Mg^{2+} ion-assisted catalytic mechanism. In most Mg^{2+}-dependent enzymes, Mg^{2+} is coordinated by 3 amino acid residues. In contrast, the crystal structure of tdEAL shows that the essential Mg^{2+} in the EAL domain is coordinated by 4 residues, presumably with high binding affinities. The mutation of any of the 4 residues rendered the enzyme almost completely inactive, indicating that they are all indispensable for Mg^{2+} binding. The coordination of the Mg^{2+} ion by the 4 residues was further confirmed by the recovery of catalytic activity for the mutants at high [Mg^{2+}] (Fig. 3). The mutation of the Glu (E_{175}) in the EXL signature motif has been known to cause inactivity in EAL domains. Our study showed that the mutation of E_{175} to either A or Q significantly reduced the enzyme activity, in agreement with the effect of the E→A mutation observed for the *V. cholerae* protein VieA (38). However, the E→Q mutation in CC3396, a GGDEF-EAL didomain protein from *C. crescentus*, did not cause significant reduction in catalytic efficiency (6). This discrepancy between RocR and CC3396 probably reflects the variation in tolerance among EAL domains.

Phosphodiesterases can catalyze the hydrolysis of substrate by using one, two, or even three metal ions. The observation of two Mg^{2+} ions in the crystal structure of tdEAL raised the possibility of a two-metal-ion catalytic mechanism, as featured in polymerases and nucleases (43). However, the mutation of the two residues (D_{296} and D_{318}) for the second Mg^{2+} ion binding caused only 29- and 8-fold reductions in the k_{cat}, suggesting that the binding of the second metal ion is not essential for catalysis. In addition, the large distance (8 Å) between the two Mg^{2+} ions rules out the possibility of a cooperative binuclear mechanism, in which the two Mg^{2+} ions are separated by a distance of ~4 Å and bridged by substrate or a Glu residue (43). Large intermetal distances have been observed for only a few enzymes, including T4 RNase H, which features an Mg^{2+}-Mg^{2+} distance of 7 Å, and T5 5′-exonuclease, which features an Mn^{2+}-Mn^{2+} distance of 8.1 Å (3, 26). Nevertheless, in both cases, solution studies suggested that only one metal ion was important for catalysis and raised the question of whether the second metal ion binding site was physiological relevant (1, 7). Given the minor impact of D296A and D318A mutations on catalysis, the observed second Mg^{2+}-binding site is likely to be a physiologically irrelevant observation resulting from the high Mg^{2+} concentration used in crystallization.

We proposed that the essential Mg^{2+} ion plays two major roles in cyclic di-GMP hydrolysis: (i) it coordinates and activates substrate by polarizing the P-O bond and (ii) it lowers the pK_a of the coordinated water to generate the nucleophilic hydroxide ion with the assistance of a general acid/base catalyst. As for the roles of D_{296} and D_{318}, considering that they are in close proximity to cyclic di-GMP, as seen in the model of the ternary complex, the decreases in k_{cat} and increases in K_m for D296A and D318A may reflect their roles in directing substrate binding. However, we cannot totally rule out a scenario in which D_{296} and D_{318} bind a labile Mg^{2+} ion, along with cyclic di-GMP.

A general base-catalyzed mechanism. Phosphodiesterases generally hydrolyze their substrates by using a metal ion(s) with the assistance of general-acid/base catalysts. A general base-catalyzed mechanism was first considered, given the large number of conserved acidic residues in the active site. Computational docking suggested that E_{352} was the primary candidate for the general base catalyst, since it is hydrogen bonded to the Mg^{2+}-coordinated H_2O molecule poised for nucleophilic attack (Fig. 5). The attack of the hydroxide ion on the electrophilic phosphorus center would generate 5′-pGpG through a trigonal bipyramid transition state common for phosphodiesterases. Although the water is probably also hydrogen bonded to D_{295}, one of the essential residues for Mg^{2+} binding, the likelihood of D_{295} acting as an efficient general base catalyst is small, since its pK_a would be considerably lowered by the Mg^{2+}. On the other hand, if E_{352} functions as the general base catalyst, we expect that the elimination of the carboxylate group by mutation would decrease the k_{cat} by more than 10^3-fold (4, 34). Indeed, the mutants E352A, E352C, and E352Q all exhibited significantly reduced activity, with a k_{cat} of $(1.1 \pm 0.1) \times 10^{-5}$ s^{-1} for the most active, E352Q. We also observed a 10^4-fold reduction in the k_{cat} for the mutant E352D, which carries the carboxylate group but with a shorter side

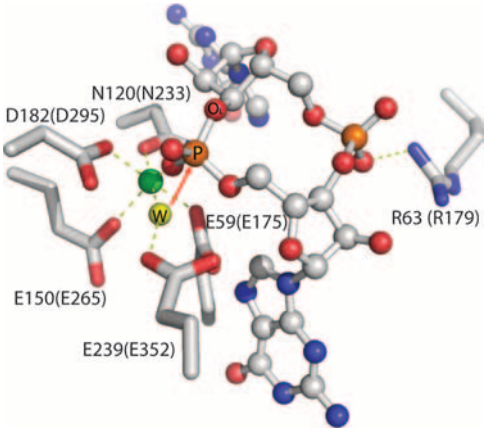

FIG. 5. Model of the tdEAL-Mg^{2+}-substrate ternary complex generated from computational docking. The residue numbers for tdEAL are shown, along with the corresponding residue numbers for EAL_{RocR} in parentheses. The water (W) (yellow ball) is coordinated by Mg^{2+} (green ball) and hydrogen bonded to E_{182} (D_{295}) and E_{239} (E_{352}) for deprotonation and nucleophilic attack. The water is positioned 3.0 Å away from the electrophilic phosphorus center, with the leaving group (O_L) aligned linearly on the opposite side of the phosphorus.

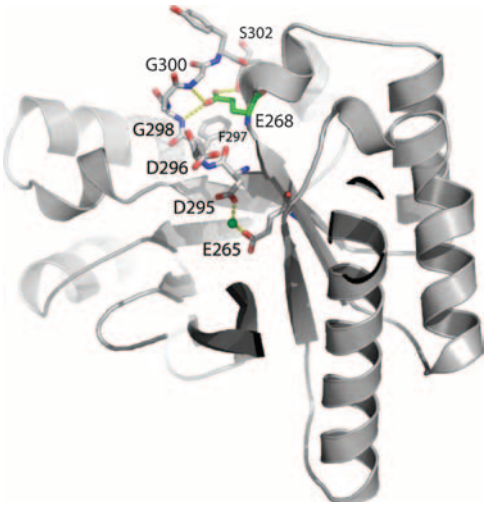

FIG. 6. Interaction between E_{268} and the loop between β5 and α6. Residues from the loop (F_{297} GAG_{300} YS_{302}), E_{268}, and the two neighboring residues (D_{295} and E_{265}) for Mg^{2+} ion (green ball) binding are highlighted to show that mutation of E_{268} may affect Mg^{2+} and substrate binding.

chain. The large decreases in k_{cat} for E352Q and E352D suggested that the precise positioning of the negatively charged carboxylate group is critical for efficient hydrolysis of cyclic di-GMP. The observed large decrease in activity caused by mutating the counterpart of E_{352} to Q in PA2567 indicates that the essential catalytic role of E_{352} is not restricted to RocR.

The notion that E_{352} functions as the general base catalyst is further supported by the pH dependence study. The significant reduction in slope for the ascending limb suggests that E_{352} largely dictates the pH dependence behavior. The change in slope supports the mechanism in which E_{352} functions as a general base and proton acceptor for deprotonating the Mg^{2+}-activated water molecule. Although the limiting slopes of 0.6 and 0.7 in the descending limb for RocR and the mutant E352Q raised the possibility of the participation of a general acid catalyst in catalysis, the involvement of a general acid catalyst is unlikely, since no suitable candidate can be identified in the active site. The observed limiting slopes in the ascending and descending limbs for the mutant may be caused by some other pH-dependent structural changes in the ternary complex.

Why is E_{268} important for catalysis? Given the distal location of the E_{268} residue, the total and partial losses of activity for mutants E268A and E268Q were initially puzzling. As seen in the structural of model of EAL_{RocR} and the crystal structure of tdEAL (2RO6), the residue E_{268} (E_{153} in tdEAL) is wrapped around by the loop connecting β6 and α6, with E_{268} hydrogen bonded to the well-conserved G_{298}, G_{300}, and S_{302} (Fig. 6). E_{268} also packs the hydrophobic region of its side chain against F_{297}, another fairly conserved residue in EAL domains. The observed interaction between E_{268} and the loop residues led us to propose that E_{268} plays an important structural role in stabilizing the loop conformation. The mutation of E_{268} may cause conformational changes in the loop and results in the dislocation of the neighboring D_{295} and D_{296}, the two conserved residues involved in Mg^{2+} and substrate binding (Fig. 6). The indirect involvement of E_{268} in Mg^{2+} binding is supported by the observation that the activity of the E268A mutant can be partially restored at high Mg^{2+} concentrations (Fig. 3). Although it remains to be seen whether E_{268} plays equally critical roles in other EAL domain proteins, the importance of E_{268} for the activity of EAL domains has been observed in at least one other protein. The EAL domain-containing YhjH from the cellulose-producing *S. enterica* serovar Typhimurium MAE97 was found to inhibit cellulose synthesis. The mutation of the corresponding residue of E_{268} to alanine in YhjH generated a mutant with stimulated cellulose biosynthesis, indicating that the mutation had a detrimental effect on the activity in vivo (33). Lastly, it is interesting to note that the DDFGTG motif proposed to be important for the activities of EAL domains contains the two residues D_{295} and D_{296}, as well as part of the loop (FGTG) discussed here (31). Given the sensitivity of the catalytic activity to the conformation of the loop, it is intriguing to speculate whether some EAL domains are regulated by changing the conformation of the loop.

Active and inactive EAL domains. EAL domains can be classified into subfamilies with different evolutionary origins according to phylogenetic analysis (20). However, it is unlikely that the subfamilies use different catalytic mechanisms because the 14 residues we examined seem to be conserved across the subfamilies. Combining the structural and biochemical data, we assigned functions to the conserved residues. Besides E_{352}, E_{268}, and the four Mg^{2+}-binding residues, K_{316} and Q_{372} are involved in the positioning of the Mg^{2+}-binding residues. R_{179} and Q_{161} are involved in substrate binding by interacting with the anionic phosphate oxygen and guanine moieties of cyclic di-GMP, respectively. The two moderately conserved residues D_{296} and D_{318} play minor roles in directing substrate binding, whereas T_{267} and E_{355} play only insignificant roles in catalysis.

If the mechanism proposed here is indeed the general catalytic mechanism for EAL domains and the identified catalytic

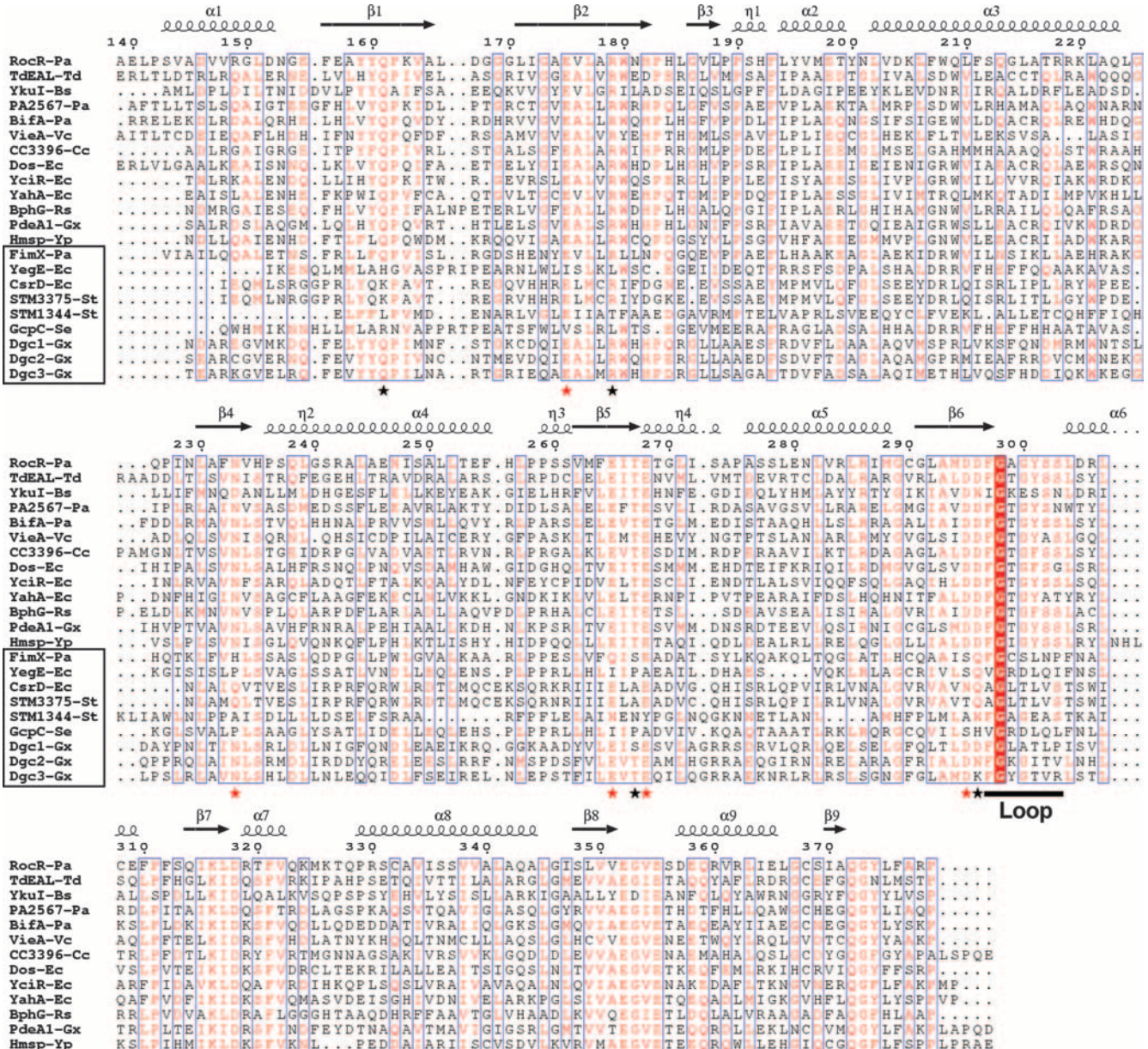

FIG. 7. Sequence alignment of the EAL domains with characterized catalytic activity. The numbering of the residues is based on the RocR sequence, and the secondary structure is based on the structure of tdEAL (PDB ID, 2R6O). EAL_{YkuI} and tdEAL are included as active EAL domains. The inactive EAL domains are shown in the boxes. The residues examined in this study are indicated by black and red asterisks (essential residues). The loop that interacts with E_{268} is underlined. Shown are PA2567, BifA, and FimX from *P. aeruginosa* (16, 19, 30); TdEAL from *T. denitrificans*; VieA from *V. cholerae* (38); CC3396 from *C. crescentus* (6); YahA, Dos, YciR, CsrD, and YegE from *E. coli* (11, 31, 35, 41); BphG from *Rhodobacter sphaeroides* (39); PdeA1, DGC1, DGC2, and DGC3 from *G. xylinus* (5, 36); HmsP from *Yersinia pestis* (2); GcpC from *S. enterica* (9); and STM1344 and STM3375 from *S. enterica* serovar Typhimurium (32). The sequences were aligned using multAlin (http://bioinfo.genopole-toulouse.prd.fr/multalin/multalin.html), and the figure was generated using Espript 2.2 (http://espript.ibcp.fr/ESPript/ESPript/).

residues are crucial for efficient hydrolysis of cyclic di-GMP, then it is logical to deduce that the EAL domains lacking one or more of these residues would be catalytically inactive or inefficient. We have experimentally confirmed the importance of E_{352} in catalysis for PA2567, a protein that contains the GGDEF-EAL didomain unit. We further examined the sequences of the EAL domains with catalytic activity characterized in either in vitro or in vivo assays. These domains are

grouped into catalytically active and inactive (or inefficient) EAL domains, as summarized in Fig. 7. All the characterized active EAL domain proteins contain the general base catalyst and Mg^{2+}-binding residues, with the exception of FimX from *P. aeruginosa* (16). Several essential residues in FimX are absent, including the corresponding residues of N_{233} (changed to H), E_{268} (changed to Q), D_{295} (changed to S), and E_{352} (changed to P). Based on our mechanism, FimX should not be able to catalyze the hydrolysis with the loss of two ligands for Mg^{2+} binding and the general base catalyst. We expressed and purified the recombinant FimX and found that it exhibited very low enzymatic activity compared to RocR (10^3- to 10^4-fold lower) (Y. Qi and Z.-X. Liang, unpublished data). Therefore, it is more appropriate to classify FimX as an inactive or inefficient EAL domain protein, given its low catalytic efficiency. Besides FimX, seven of the other eight inactive EAL domains lack one or more of the essential residues. Notably, all seven of them do not contain a Glu at the corresponding E_{352} position. The EAL domain of the inactive CsrD was proposed to play a role other than hydrolyzing cyclic di-GMP (35). Examination of the sequences of the homologous proteins of CsrD showed that none of them contains Glu at the corresponding position of E_{352} (35). The only "inactive" EAL domain that cannot be rationalized is DGC2, which contains all the essential residues and should be a functional phosphodiesterase domain. Note that the protein contains a GGDEF domain and a regulatory PAS domain that may suppress the activity of the EAL domain under the assay conditions (36). Studies are being conducted in our laboratory to examine the in vitro activities of DGC2 and some other EAL domain proteins lacking one or more of the essential catalytic residues.

These results indicate that the absence of the essential catalytic residues can serve as markers for identifying catalytically inactive EAL domains in the bacterial genomes. This has great implications, considering that more than 20% of the EAL domains in bacterial genomes harbor a different residue at the position corresponding to the previously unrecognized E_{352} site. Given the large number of inactive EAL domains predicted based on this method, the elucidation of the functions of these EAL domains presents a new challenge in understanding cyclic di-GMP signaling.

Physiological function of RocR. The cyclic di-GMP cellular concentrations in *C. crescentus* and *A. xylinum* have been estimated to be 1.2 μM and 5 to 10 μM, respectively (6, 42). The cellular concentration of cyclic di-GMP in *P. aeruginosa* is likely to be on the same order of magnitude, considering that the dissociation constant for one of the cyclic di-GMP binding proteins in *P. aeruginosa* is 8.4 μM (24). Furthermore, the observed K_m (3.3 ± 0.3 μM) for RocR is larger than the K_m (0.42 μM) for the activated CC3396 from *C. crescentus*, indicating that RocR is probably in its inactive state for cyclic di-GMP hydrolysis under physiological conditions. The phosphorylation of the N-terminal CheY-like domain may activate the EAL domain by altering K_m and alter its binding affinity for the cognate histidine kinase RocS1. It was initially implied that the EAL_{RocR} domain may function as a regulatory domain rather than a catalytic domain and that its role is to regulate the binding affinity of the CheY domain for the histidine kinase RocS1 (21). Given the observed catalytic activity of the EAL_{RocR} domain, the model in which RocR competes with RocA for phosphoryl transfer from RocS1 seems to be more suitable (18). Considering that RocA regulates the transcription of virulence genes and that cyclic di-GMP regulates biofilm formation and other multicellular behaviors, it is conceivable that the RocSAR system may function as a switch system controlling different phenotypes in *P. aeruginosa*, which is known for its extraordinary ability to adapt to the surrounding environment. The proteins homologous to RocR, including SadR from *P. aeruginosa* PA14, VieA from *V. cholerae*, and BvgR from *B. pertussis*, may play similar roles controlling the phenotype switch that is crucial for in vivo survival and infection (18, 25, 38).

ACKNOWLEDGMENTS

This work is supported by the Singapore Biomedical Research Council through a BMRC grant (06/1/22/19/464) and the Ministry of Education of Singapore through a URC grant (RG151/06).

We thank Tang Kai for his assistance with our mass spectrometry experiments.

REFERENCES

1. **Black, C. B., and J. A. Cowan.** 1998. A critical evaluation of metal-promoted Klenow 3′-5′ exonuclease activity: calorimetric and kinetic analyses support a one-metal-ion mechanism J. Biol. Inorg. Chem. **3:**292–299.
2. **Bobrov, A. G., V. Kirillina, and R. D. Perry.** 2007. Regulation of biofilm formation in *Yersinia pestis*. Adv. Exp. Med. Biol. **603:**201–210.
3. **Ceska, T. A., J. R. Sayers, G. Stier, and D. Suck.** 1996. A helical arch allowing single-stranded DNA to thread through T5 5′-exonuclease. Nature **382:**90–93.
4. **Cha, J., and D. S. Auld.** 1997. Site-directed mutagenesis of the active site glutamate in human matrilysin: investigation of its role in catalysis. Biochemistry **36:**16019–16024.
5. **Chang, A. L., J. R. Tuckerman, G. Gonzalez, R. Mayer, H. Weihouse, G. Volman, D. Amikam, M. Benziman, and M. A. Gilles-Gonzalez.** 2001. Phosphodiesterase A1, a regulator of cellulose synthesis in *Acetobacter xylinum*, is a heme-based sensor. Biochemistry **40:**3420–3426.
6. **Christen, M., B. Christen, M. Folcher, A. Schauerte, and U. Jenal.** 2005. Identification and characterization of a cyclic di-GMP-specific phosphodiesterase and its allosteric control by GTP. J. Biol. Chem. **280:**30829–30837.
7. **Cowan, J. A.** 1998. Metal activation of enzymes in nucleic acid biochemistry. Chem. Rev. **98:**1067–1087.
8. **Dolinsky, T. J., J. E. Neilsen, J. A. MacCammon, and N. A. Baker.** 2004. PDB2PQR: an automated pipeline for the setup of Poisson-Boltzmann electrostatics calculations. Nucleic Acids Res. **32:**665–667.
9. **Garcia, B., C. Latasa, C. Solano, F. G. Portillo, C. Gamazo, and I. Lasa.** 2004. Role of the GGDEF protein family in *Salmonella* cellulose biosynthesis and biofilm formation. Mol. Microbiol. **54:**264–277.
10. **Garrett, G. M., D. S. Goodsell, R. S. Halliday, R. Huey, W. E. Hart, R. K. Belew, and A. J. Olson.** 1998. Automated docking using a Lamarckian genetic algorithm and an empirical binding free energy function. J. Comput. Chem. **19:**1639–1662.
11. **Girgris, H. S., Y. Liu, W. S. Ryu, and S. Tavazoie.** 2007. A comprehensive genetic characterization of bacterial motility. PLoS Genet. **3:**1644–1660.
12. **Hisert, K. B., M. MacCoss, M. U. Shiloh, K. H. Darwin, S. Singh, R. A. Jones, S. Ehrt, Z. Y. Zhang, B. L. Gaffney, S. Gandotra, D. W. Holden, D. Murray, and C. Nathan.** 2005. A glutamate-alanine-leucine (EAL) domain protein of *Salmonella* controls bacterial survival in mice, antioxidant defense and killing of macrophages: role of cyclic di-GMP. Mol. Microbiol. **56:**1234–1245.
13. **Huang, B., C. B. Whitchurch, and J. S. Mattick.** 2003. FimX, a multidomain protein connecting environmental signals to twitching motility in *Pseudomonas aeruginosa*. J. Bacteriol. **185:**7068–7076.
14. **Jenal, U., and J. Malone.** 2006. Mechanisms of cyclic-di-GMP signaling in bacteria. Annu. Rev. Genet. **40:**385–407.
15. **Karatan, E., T. R. Duncan, and P. I. Watnick.** 2005. NspS, a predicted polyamine sensor, mediates activation of *Vibrio cholerae* biofilm formation by norspermidine. J. Bacteriol. **187:**7434–7443.
16. **Kazmierczak, B. I., M. B. Lebron, and T. S. Murray.** 2006. Analysis of FimX, a phosphodiesterase that governs twitching motility in *Pseudomonas aeruginosa*. Mol. Microbiol. **60:**1026–1043.
17. **Kim, Y.-K., and L. L. McCarter.** 2007. ScrG, a GGDEF-EAL protein, participates in regulating swarming and sticking in *Vibrio parahaemolyticus*. J. Bacteriol. **189:**4094–4107.
18. **Kuchma, S., J. P. Connolly, and G. A. O'Toole.** 2005. A three-component regulatory system regulates biofilm maturation and type III secretion in *Pseudomanas aeruginosa*. J. Bacteriol. **187:**1441–1454.

19. **Kuchma, S. L., K. M. Brothers, J. H. Merritt, N. T. Liberati, F. M. Ausubel, and G. A. O'Toole.** 2007. BifA, a cyclic-di-GMP phosphodiesterase, inversely regulates biofilm formation and swarming motility by *Pseudomonas aeruginosa* PA14. J. Bacteriol. **189:**8165–8178.
20. **Kulasakara, H., V. Lee, A. Brencic, N. Liberati, J. Urbach, S. Miyata, D. G. Lee, A. N. Neely, M. Hyodo, Y. Hayakawa, F. M. Ausubel, and S. Lory.** 2006. Analysis of *Pseudomonas aeruginosa* diguanylate cyclases and phosphodiesterases reveals a role for bis-(3′-5′)-cyclic-GMP in virulence. Proc. Natl. Acad. Sci. USA **103:**2839–2844.
21. **Kulasekara, H. D., I. Ventre, B. R. Kulasekara, A. Lazdunski, A. Filloux, and S. Lory.** 2005. A novel two-component system controls the expression of *Pseudomonas aeruginosa* fimbrial cup genes. Mol. Microbiol. **55:**368–380.
22. **Li, H., A. D. Robertson, and J. H. Jensen.** 2005. Very fast empirical prediction and rationalization of protein pK_a values. Protein Sci. **61:**704–721.
23. **Lim, B., S. Beyhan, J. Meir, and F. H. Yildiz.** 2006. Cyclic-di-GMP signal transduction systems in *Vibrio cholerae*: modulation of rugosity and biofilm formation. Mol. Microbiol. **60:**331–348.
24. **Merighi, M., V. T. Lee, M. Hyodo, Y. Hayakawa, and S. Lory.** 2007. The second messenger bis-(3′-5′)-cyclic-GMP and its PilZ domain-containing receptor Alg44 are required for alginate biosynthesis in *Pseudomonas aeruginosa*. Mol. Microbiol. **65:**876–895.
25. **Merkel, T. J., S. Stibitz, J. M. Keith, M. Leef, and R. Shahin.** 1998. Contribution of regulation by the *bvg* locus to respiratory infection of mice by *Bordetella pertussis*. Infect. Immun. **66:**4367–4373.
26. **Mueser, T. C., N. G. Nossal, and C. C. Hyde.** 1996. Structure of bacteriophage T4 RNase H, a 5′ to 3′ RNA-DNA and DNA-DNA exonuclease with sequence similarity to the RAD2 family of eukaryotic proteins. Cell **85:**1101–1112.
27. **Romling, U., M. Gomelsky, and M. Y. Galperin.** 2005. C-di-GMP: the dawning of a novel bacterial signaling system. Mol. Microbiol. **57:**629–639.
28. **Ross, P., R. Mayer, H. Weinhouse, D. Amikam, Y. Huggirat, M. Benziman, E. de Vroom, A. Fidder, P. de Paus, and L. A. Sliedregt.** 1990. The cyclic diguanylic acid regulatory system of cellulose synthesis in *Acetobacter xylinum*. Chemical synthesis and biological activity of cyclic nucleotide dimer, trimer, and phosphothioate derivatives. J. Biol. Chem. **265:**18933–18943.
29. **Ruer, S., S. Stender, A. Filloux, and S. de Bentzmann.** 2007. Assembly of fimbrial structures in *Pseudomonas aeruginosa*: functionality and specificity of chaperone-usher machineries. J. Bacteriol. **189:**3547–3555.
30. **Ryan, R. P., Y. Fouhy, J. F. Lucey, L. C. Crossman, S. Spiro, Y.-W. He, L.-H. Zhang, S. Heeb, M. Camara, P. Williams, and J. M. Dow.** 2006. Cell-cell signaling in *Xanthomonas campestris* involves an HD-GYP domain protein that functions in cyclic di-GMP turnover. Proc. Natl. Acad. Sci. USA **103:**6712–6717.
31. **Schmidt, A. J., D. A. Ryjenkov, and M. Gomelsky.** 2005. The ubiquitous protein domain EAL is a cyclic diguanylate-specific phosphodiesterase: enzymatically active and inactive EAL domains. J. Bacteriol. **187:**4774–4781.
32. **Simm, R., A. Lusch, A. Kader, M. Andersson, and U. Romling.** 2007. Role of EAL-containing proteins in multicellular behavior of *Salmonella enterica* serovar Typhimurium. J. Bacteriol. **189:**3613–3623.
33. **Simm, R., M. Morr, A. Kader, M. Nimtz, and U. Romling.** 2004. GGDEF and EAL domains inversely regulate cyclic-di-GMP levels and transition from sessility to motility. Mol. Microbiol. **53:**1123–1134.
34. **Stanford, N. P., S. E. Halford, and G. S. Baldwin.** 1999. DNA cleavage by the EcoRV restriction endonuclease: pH dependence and proton transfers in catalysis. J. Mol. Biol. **288:**105–116.
35. **Suzuki, K., P. Babitzke, S. R. Kushner, and T. Romeo.** 2006. Identification of a novel regulatory protein (CsrD) that targets the global regulatory RNAs CsrB and CsrC for degradation by RNase E. Genes Dev. **20:**2605–2617.
36. **Tal, R., H. C. Wong, R. Calhoon, D. Gelfand, A. L. Fear, G. Volman, R. Mayer, P. Ross, D. Amikam, H. Weinhouse, A. Cohen, S. Sapir, P. Ohana, and M. Benziman.** 1998. Three *cdg o*perons control cellular turnover of cyclic di-GMP in *Acetobacter xylinum*: genetic organization and occurrence of conserved domains in isoenzymes. J. Bacteriol. **180:**4416–4425.
37. **Tamayo, R., J. T. Pratt, and A. Camilli.** 2007. Roles of cyclic diguanylate in the regulation of bacterial pathogenesis. Annu. Rev. Microbiol. **61:**131–148.
38. **Tamayo, R., A. D. Tischler, and A. Camilli.** 2005. The EAL domain protein VieA is a cyclic diguanylate phosphodiesterase. J. Biol. Chem. **280:**33324–33330.
39. **Tarutina, M., D. A. Ryjenkov, and M. Gomelsky.** 2006. An unorthodox bacteriophytochrome from *Rhodobacter sphaeroides* involved in turnover of the second messenger c-di-GMP. J. Biol. Chem. **281:**34751–34758.
40. **Tischler, A. D., and A. Camilli.** 2004. Cyclic diguanylate (c-di-GMP) regulates *Vibrio cholerae* biofilm formation. Mol. Microbiol. **53:**857–869.
41. **Weber, H., C. Persavento, G. Possling, G. Tischendorf, and R. Hengge.** 2006. Cyclic-di-GMP-mediated signaling within the σ^S network of *Escherichia coli*. Mol. Microbiol. **62:**1014–1034.
42. **Weinhouse, H., S. Sapir, D. Amikam, Y. Shilo, G. Volman, P. Ohana, and M. Benziman.** 1997. C-di-GMP-binding protein, a new factor regulating cellulose synthesis in *Acetobacter xylinum*. FEBS Lett. **416:**207–211.
43. **Yang, W., J. Y. Lee, and M. Nowotny.** 2006. Making and breaking nucleic acids: Two-$Mg2^+$ catalysis and substrate specificity. Mol. Cell **22:**5–13.
44. **Zhang, Z., B. L. Gaffney, and R. A. Jones.** 2004. C-di-GMP displays a monovalent metal ion-dependent polymorphism. J. Am. Chem. Soc. **126:**16700–16701.